[1] A. Pavithra
[1*]G. Kalpana

Deep Learning Enabled Efficient Net with KLM for Pragmatic Plant Disease Diagnosis

JES Journal of Electrical Systems

Abstract: - Research is still being done on the automated identification and classification of plant diseases. A quick and precise methodology for identifying plant diseases can improve both small-scale commercial crop protection and large-scale food security. Deep learning (DL) methods also enable the monitoring of plant health and the early diagnosis of illnesses. This study's DLEN-KLM model, which is built on EfficientNet and Kernel extreme Learning Machine (KLM) and is designed to diagnose plant diseases intelligently, addresses this issue. In contrast to limited adaptive histogram equalisation as a preprocessing method, the suggested DLEN-KLM model uses median filtering in its construction. A feature extractor built on EfficientNet B0 is also part of the DLEN-KLM model, which is used to create the best feature vectors before categorising them with the KLM model. Utilising a benchmark dataset, the effectiveness of the DLEN-KLM technique is validated. The experimental results showed that the technique outperformed more contemporary methods in terms of disease diagnosis.

Keywords: Median filtering, Adaptive histogram equalization, KLM classifier, Deep learning, EfficientNet model.

I. INTRODUCTION

The Indian economy is heavily reliant on agricultural production [1]. Thus, in fields of agriculture, detecting diseases in plant play a significant part. In order to discover plant diseases in an earlier phase, usage of automated disease detection techniques is highly useful. The diseased trees barely recover and die within six to seven years [2, 3]. Georgia and Alabama, both in the Southern US, have seen its effects. An early diagnosis may be helpful in this case. Emerging methods for detecting and mitigating plant diseases serve the dual purposes of lowering pesticide use and boosting food productivity, with estimates for the world's population to reach 10 billion by 2055 [4]. The primary goal of achieving food safety, in addition to the development of better crop varieties, is the detection of diseases. The traditional techniques of disease detection have involved expert/farmer manual checks that are expensive and time-consuming, proving to be unworkable for millions of farms worldwide [5].

The traditional model for detecting plant diseases is just naked eye observation by specialists whereby detection and identification of plant disease are performed. In this regard, a continuous monitoring and large team of experts of plants are needed that are very expensive. Simultaneously, in many countries, farmers don’t have appropriate facilities or even idea that they might interact with the expert. Consequently, consulting experts time consuming and high cost [6]. Detecting Plant disease through visual manner is less accurate and simultaneously, more laborious task and only made in constrained regions. Where automated detection techniques are employed, it might take less time, less efforts also become higher precision. Image processing is used to assess diseased regions that are infected and to ascertain how the colours of such regions vary [7]. Support machine vision is also used to provide image-based robot guiding, inspection, automation, and control [8].

There has been a significant rise in research into computer vision models to enhance automatic approaches for recognising plant diseases with evident symptoms on leaves. As much farmer and detection system input as possible is being sought after by this system. Prior to the easier accessibility of deep learning models, research primarily focuses on using feature extraction to enhance technique for diagnosing diseases with variable outcomes. Artificial intelligence (AI), computer vision, and machine learning have all benefited several applications, including power forecasts for medicinal and renewable resource applications. AI has been extensively used in the COVID19 epidemic for the diagnosis of lung disorders and other predictive applications [9]. Through earlier diagnosis and detection, modern technologies can be used to lessen the detrimental effects of plant diseases. The automated diagnosis and detection of plant disease using computer vision and artificial intelligence (AI) is currently a hot topic of research due to the time-consuming, labor-intensive, and boring nature of autonomous monitoring of plant diseases.

[1,1*]Department of Computer Science, Faculty of Science and Humanities, SRM Institute of Science and Technology, Kattankulathur, 603203

kalpanag@srmist.edu.in, pa6635@srmist.edu.in

The deep transfer learning-based EfficientNet and Kernel ExtremeLearning Machine (KLM) model called DLEN-KLM was created in this study. The suggested DLEN-KLM model employs both the median filtering (MF) method of noise removal and the contrast limited adaptive histogram equalisation (CLAHE) approach of contrast enhancement. The DLEN-KLM model also uses an EfficientNet B0 based feature extractor to produce the best feature vectors, which are subsequently classified using the KLM model.

II. RELATED WORKS

Hernández and Lopez [10] developed a probabilistic programming method for detecting plant diseases through advanced Bayesian DL methods and the ambiguity as misclassification measurements . The result shows that Bayesian inference attains classification accuracy i.e., related with the benchmark optimization procedure to finetune DL methods. Guo et al. [11] proposed an arithmetical method of plant disease recognition and detection on the basis of DL method that enhances training efficiency, accuracy, and generality. First, the RPN has been employed to localize and recognize the leaf in complicated surroundings. Next, image segments depend on the result of RPN have the features of symptom via CV model. Lastly, the segmented leaf is inputted to the TL models and trained with the datasets of diseased leaves in simple background.

In Saleem et al. [12], 3 DL Meta architecture includes SSD, Fast RCNN, and RFC have been used with the help of TensorFlow object detection frameworks. Each DL model is tested or trained on controllable environmental datasets for recognizing the diseases in plant species. Furthermore, an enhancement in the mean average accuracy of the optimally attained DL framework has been tried via an advanced DL optimizer. Kabir et al. [13] investigate an optimum plant disease detection method intergrading the diagnoses of many plants. In spite of being based on multiclass classifications, the method inherits multilabel classification methods for identifying the plant and the kind of diseases separately. For the evaluation and experiment, they have gathered information from different online sources which include leaf images of 6 plants, involving potato, tomato, corn, rice, apple, and grape.

In Hong et al.'s [14] research, transfer learning has been used to decrease the amount of training data required as well as the time and cost associated with processing it. Patil and Patil [15] are conducting research to manually identify diseased plants using cotton plant leaf photos. Additionally, an Internet of Things-based framework is being utilized to collect various sensor information in order to identify climate fluctuations. By collecting photos through the full technique used in validation and training for image augmentation, fine-tuning, and pre-processing, the DCNN models are proposed for conducting cotton plant disease identification through healthy and infected cotton leaf images. This is accomplished by gathering images.

Lijo [16] analyzes 3 main TL methods i.e. ResNet50, InceptionV3and DenseNet169 with an augmentation and with no augmentation for image classifications and thus detecting plant diseases. Afterward employing the abovementioned methods they examined the efficacy through different quality metrics: recall, precision, F1-score, accuracy. Turkoglu et al. [17] proposed 2 classification methods on the basis of deep feature extraction from pretrained CNN. In the proposed models, also they finetune and integrate 6 advanced CNN and calculate the provided problems as ensemble and individually. Lastly, the performance of distinct combinations depends on the presented method is estimated by an SVM classifier.

III. PROPOSED MODEL

This study develops a novel DLEN-KLM model for identifying and categorising plant diseases. The Median filtering-based noise removal, Limited adaptive histogram equalisation -based contrast enhancement, Otsu thresholding-based segmentation, EfficientNet B0-based feature extraction, and KLM-based classification are some of the various subprocesses that together forms the DLEN-KLM model. The complete operation of the DLEN-KLM model is shown in Fig. 1.

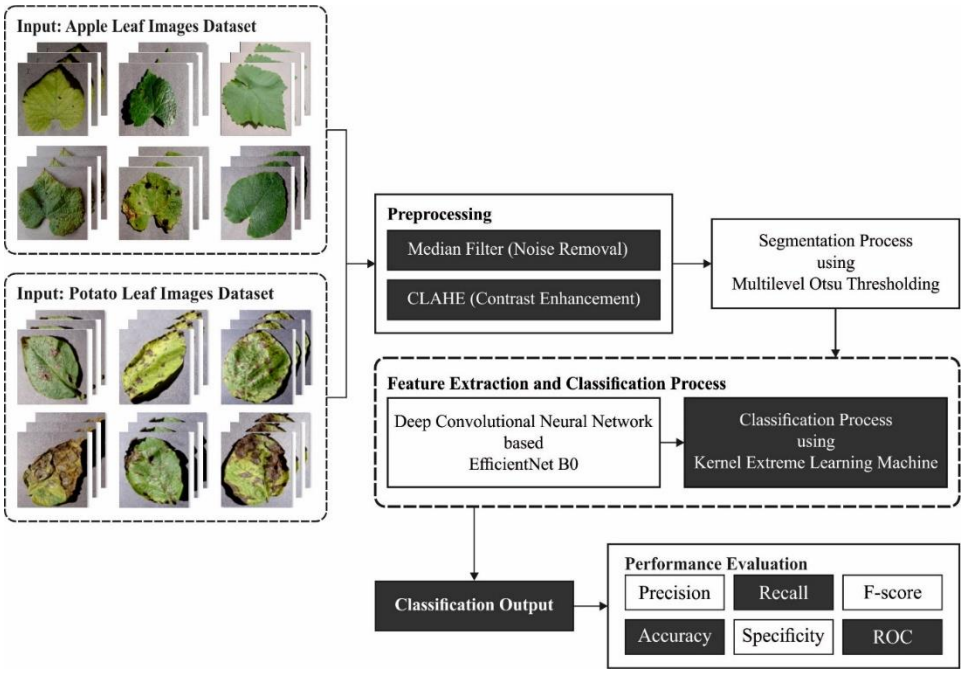

Figure 1. Overview of DLEN-KLM model

3.1. Noise removal and Contrast enhancement in Image Preprocessing

The preprocessing is done in two levels at the main stage: Median filter based noise removal and CLAHE-based contrast enhancement. The Median filter is a method of non-linear signal processing that relies on statistics. The output of the Median filter is g(u,v)=medf(u-i,v-j),i,jW, where f(u,v), g(u,v) signify both the source and the result pictures, and W denotes the 2Dimentional mask. The mask size is nn (whereas n is generally odd), such as 3*3,5*5. Because the Median filter uses a non-linear filter, their mathematical analysis is more difficult for images with arbitrary noise. [18]

$$\sigma_{med}^2 = \frac{1}{4nf^2(\overline{n})} \approx \frac{\sigma_i^2}{n + \frac{\pi}{2} - 1} \cdot \frac{\pi}{2}. \qquad (1)$$

Whereas σ_i^2 denotes the variation, n represents the size of Median filter mask, $f(\bar{n})$ indicates the function of noise density. Also, the variance of the normal filter can be given below

$$\sigma_0^2 = \frac{1}{n}\sigma_k^2. \qquad (2)$$

The Adaptive Histogram Equalisation (AHE) technique is modified by the CLAHE. To perform equalisation in various regions of the image. Bilinear interpolation is used to correct irregularities in the borders. The CLAHE was created because the AHE has a problem with noise amplification. It restricts the number of pixels that can be used to create particular grey scales.

3.2. Using Multi-level Otsu thresholding Technique in Image Segmentation :

Using the multi-level Otsu thresholding approach, the preprocessed image is segmented to identify the infected and healthy areas. Consider the pixels in a picture that are shown to exist in L different grayscales (1, 2,..., L). Assume that N represents the total number of pixels and n_i is the count of pixels at level i, with $N = \sum_{i=1}^{L} n_i$. Assuming that pi=niN, we may calculate the level i probability of occurrence.Z-threshold is taken into consideration when dividing a picture into the classes C0 and C1. The levels [1, Z] are present in pixels in C0, while levels [Z+1, L] are present in pixels in C1. It is assumed that P0(Z) and P1(Z) reflect the cumulative probability, that $\mu_0(Z)$ and $\mu_1(Z)$ indicates the level of mean , and $\sigma_0^2(Z)$ and $\sigma_1^2(Z)$ denote the class variances C0 and C1, respectively. We supply these values as:

$$P_0(Z) = \sum_{i=1}^{Z} p_i \quad (3)$$

$$P_1(Z) = \sum_{i=Z+1}^{L} p_i = 1 - P_0(Z) \quad (4)$$

$$\mu_0(Z) = \sum_{i=1}^{Z} i \frac{p_i}{P_0(Z)} = \frac{1}{P_0(Z)} \sum_{i=1}^{Z} i\, p_i \quad (5)$$

$$\mu_1(Z) = \sum_{i=Z+1}^{L} i \frac{p_i}{P_1(Z)} = \frac{1}{P_1(Z)} \sum_{i=Z+1}^{L} i\, p_i \quad (6)$$

$$\sigma_0^2(Z) = \sum_{i=1}^{Z} (i - \mu_0(Z))^2 \frac{p_i}{P_0(Z)} \quad (7)$$

$$\sigma_1^2(Z) = \sum_{i=Z+1}^{L} (i - \mu_1(Z))^2 \frac{p_i}{P_1(Z)} \quad (8)$$

Supposed μ, $\sigma_b^2(Z)$, and $\sigma_w^2(Z)$ demonstrated the mean level of image, within-class variance and the between-class variance, correspondingly [19]:

$$\mu = \sum_{i=1}^{L} i\, p_i = P_0(Z)\mu_0(Z) + P_1(Z)\mu_1(Z) \quad (9)$$

$$\sigma_b^2(Z) = P_0(Z)(\mu_0(Z) - \mu)^2 + P_1(Z)(\mu_1(Z) - \mu)^2 \quad (10)$$

$$\sigma_w^2(Z) = P_0(Z)\sigma_0^2(Z) + P_1(Z)\sigma_1^2(Z) \quad (11)$$

The limit demonstrated by maximising the between-class variance provided by Otsu is:

$$Z^* = \underset{1 \le Z < L}{\arg}\ \text{maxi}\, \{\sigma_b^2(Z)\} \quad (12)$$

This value is similar to the threshold determined by the principle of minimised within-class variances.:

$$Z^* = \underset{1 \le Z < L}{\arg}\ \text{mini}\, \{\sigma_w^2(Z)\} \quad (13)$$

3.3. Feature Extraction using EfficientNet :

A collection of vectors are extracted by the EfficientNet B0 model from the segmented image during feature extraction. Eight models make up the EfficientNet group, which is divided into B0 and B7. As the number of models increases, the number of variables that are evaluated does not, but accuracy does, with a dramatic increase. Instead of the Rectifier Linear Unit (ReLU) activation function, EfficientNet implements a unique activation function called Swish [20]. DL architecture aims to reveal tiny, effective solutions with efficient approaches. By consistently scaling the models' width, resolution, and depth as they are shrunk, EfficientNet, unlike another sophisticated technique, produces efficient results. The compound scaling model initially looks for a grid in order to discover correlations between the various scaling parameters of the baseline network within preset resource restrictions. Using this coefficient, the baseline network is later scaled to the selected target networks. In Fig. 2, the EfficientNet model's architecture is shown. Direct connection is used between bottlenecks in MBConv because the block comprises a layer that expands and then contracts the channel initially. The compression layer connects a lot fewer channels than the expansion layer does. When compared to a traditional layer, this framework's in-depth separable convolution reduces estimates by a factor of k2 while k stands for the kernel size, which specifies the height and width of the two-dimensional convolutional windows.

Stage	Operator	Resolution	#Channels	#Layers
1	Conv3x3	224 x 224	32	1
2	MBConv1, k3x3	112 x 112	16	1
3	MBConv6, k3x3	112 x 112	24	2
4	MBConv6, k5x5	56 x 56	40	2
5	MBConv6, k3x3	28 x 28	80	3
6	MBConv6, k5x5	14 x 14	112	3
7	MBConv6, k5x5	14 x 14	192	4
8	MBConv6, k3x3	7 x 7	320	1
9	Conv1x1 and Pooling and FC	7 x 7	1280	1

Figure. 2. Efficient Net Architecture

When scaling resolution, depth, and width uniformly, the compound coefficients (as indicated in Eq. 14) are used under the principle of compound scaling.

$$depth: d = \alpha^{\psi}$$
$$width: w = \beta^{\psi} \quad (14)$$
$$resolution: r = \gamma^{\psi}$$
$$\alpha \geq 1, \beta \geq 1, \gamma \geq 1$$

Contrarily, the grid search's definition of a constant is represented by the notation α, β, γ. The user-determined coefficients shown by the symbol regulate how much resource is available for model scaling, whereas the symbols,, dictate how these extra resources are assigned to the network's resolution, width, and depth, respectively. FLOPS is inversely correlated to d, w^2, r^2 in a popular convolutional technique. Scaling convolutional networks as shown in Eq. (14) increases the network's FLOPSs (floating point operation per second) by an average of $(\alpha, \beta^2, \gamma^2)^{\phi}$ $(\alpha. \beta^2 y^2)^{\phi}$. This is because convolutional operations account for the majority of the convolutional network's processing cost.The compound scaling methods scale these models in two steps as follows:

Step1: Grid searching is carried out by $\phi = 1$ and assumes that there are twice as many resources available. Also the ideal values are chosen for α, β, γ.

Step2: The baseline networks scale up in order to obtain EffcientNetB1 to B7 with distinct ϕ value by Eq. (14). Obtain α, β, γ values are defined as constants. EfficientNet B0 model is employed in this study's feature extraction technique.

3.4. KLM Technique based Image Classification

The feature vectors extracted from feature extraction are supplied as input to the KLM model to assign the proper class labels at the time of final picture classification. ELM was first proposed using the FFNN model. The KLM model's structure is depicted in Fig. 3. Determine $y_k \in \{0,1\}, 1 \leq k \leq C$ for the C class. The class a sample belongs to is indicated by the row vector $y = [y_1, \dots, y_k \dots, y_C]$. For instance, the samples fall into the kth classes when $y_k = 1$ and the remaining parts of y are 0. Assuming that P training sample $\{x_i, y_i\}_{i=1}^{P}$ belongs to the C class and that $x_i \in R^N$ & $y_i \in R^C$, respectively, the output function of ELM possessing L hidden neuron might be given by

$$f(x_i) = \sum_{j=1}^{L} \beta_j \, h(\omega_j \cdot x_i + e_j) = y_i, i = 1, \dots, P \quad (15)$$

The terms h(.) describe a non-linear activation function (such as a Sigmoid function), $\beta_i \in R^C$ represent the weight vector connecting jth output and hidden neurons [21], $\omega_j \in R^N$means the weight vector connecting jth input and hidden neurons, and e_j defines the bias of jth hidden neurons. The inner product of ω_j. and $x_i$is represented as $\omega_j \cdot x_i$.

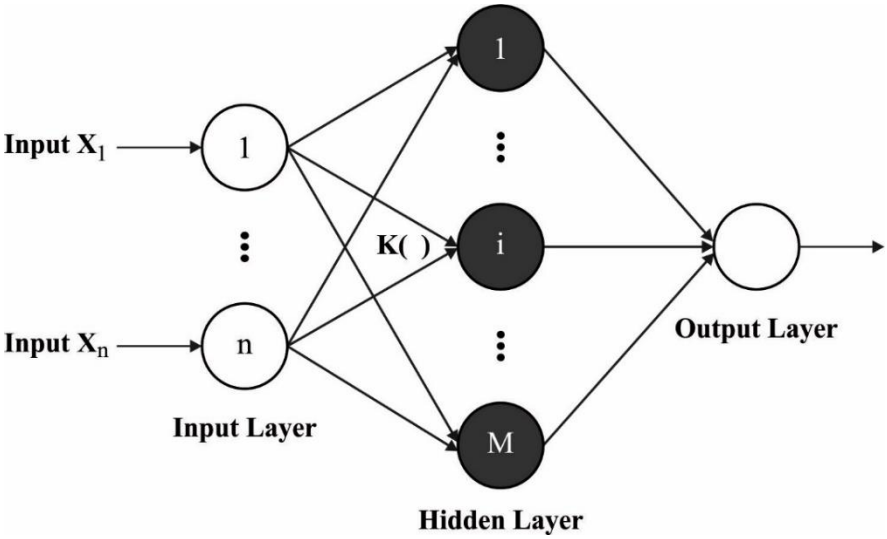

Figure 3. KLM architecture

With *P* equation, Eq. (15) could be expressed by

$$\beta = Y \qquad (16)$$

whereas $= [y_1^T y_2^T \dots y_P^T]^T \in R^{P\times C}$, $\beta = [\beta_1^T \beta_2^T \dots \beta_L^T]^T \in R^{L\times C}$, and H denotes the hidden layer output matrix of NN:

$$H = \begin{bmatrix} h(x_1) \\ \vdots \\ h(x_P) \end{bmatrix} = \begin{bmatrix} h(\omega_1 \cdot x_1 + e_1) & \cdots & h(\omega_L \cdot x_1 + e_L) \\ \vdots & \ddots & \vdots \\ h(\omega_1 \cdot x_P + e_1) & \cdots & h(\omega_L \cdot x_P + e_L) \end{bmatrix}_{P\times L} \qquad (17)$$

$H(x_i) = (h(\omega_1 \cdot x_1 + e_1), \dots, h(\omega_L \cdot x_1 + e_L))$ is the result of hidden neurons that transfer the data from N-dimensional input space to L-dimensional feature space, with respect to the input x_i. As a result of the fact that there are always less hidden neurons than training examples, or P, the smaller norm least square solution of Eq. (16) is established by

$$\beta' = H^{\dagger} Y \qquad (18)$$

While H denotes matrix H's Moore-Penrose generalisation inverse. $H^{\dagger} = H^T (HH^T)^{-1}$ could be used to determine the Moore-Penrose generalisation inverse of H. Positive values $\frac{1}{\rho}$ are included in the diagonal element of HH^T for greater generalisation and stability.

$$f(x_i) = h(x_i)\beta = h(x_i)H^T \left(\frac{I}{\rho} + HH^T\right) Y \qquad (19)$$

A user of ELM is often aware of a feature mapping called $h(x_i)$. The kernel matrix for ELM could be determined by the user when a feature mapping is unknown.:

$$\Omega_{ELM} = HH^T : \Omega_{ELM_{q,t}} = h(x_q) \cdot h(x_t) = K(x_q, x_t) \qquad (20)$$

Thus, KLM output is expressed is expressed by

$$f(x_i) = h(x_i)H^T \left(\frac{I}{p} + HH^T\right)^{-1} Y = \begin{bmatrix} K(x_i, x_1) \\ \vdots \\ K(x_i, x_P) \end{bmatrix}^T \left(\frac{I}{p} + \Omega_{ELM}\right)^{-1} Y \qquad (21)$$

The index of the output node with the highest values has been defined as the label of the input data.

IV. EXPERIMENTAL VALIDATION

In this section, the effectiveness of the suggested method is examined by Apple plant disease and potato plant disease datasets [22]. It includes a number of instances under different classes. The dataset contains a set of 1000 images under each dataset. Python 3.6.5 is used as a tool to simulate the stated technique.

4.1. Results of the Dataset on Apple Plant Disease

The proposed model's results analysis on the used dataset for apple pant disease are examined in this section. Test picture samples from the dataset are shown in Fig. 4.

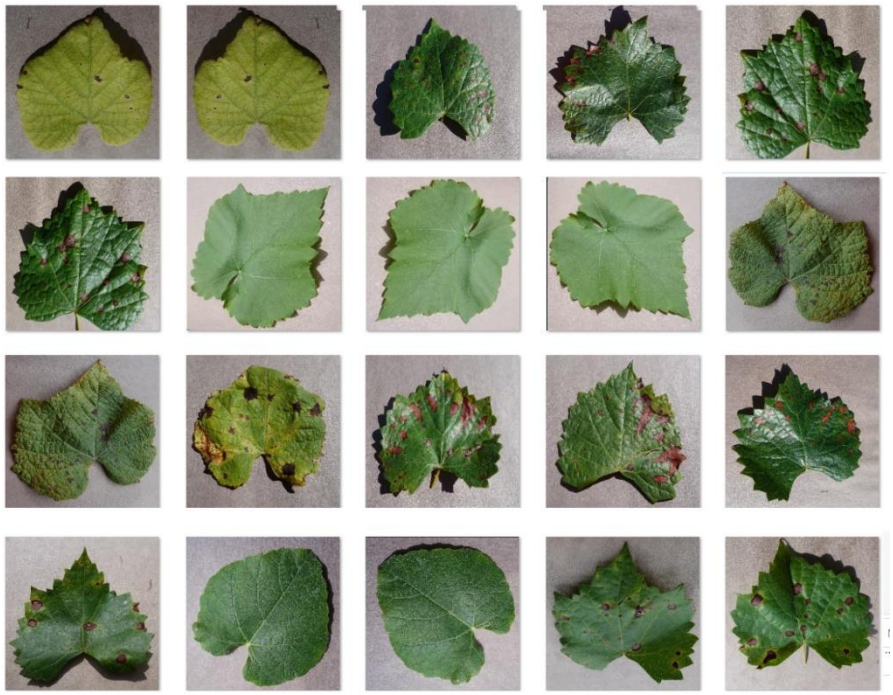

Figure 4. Sample Apple Plant Disease Images

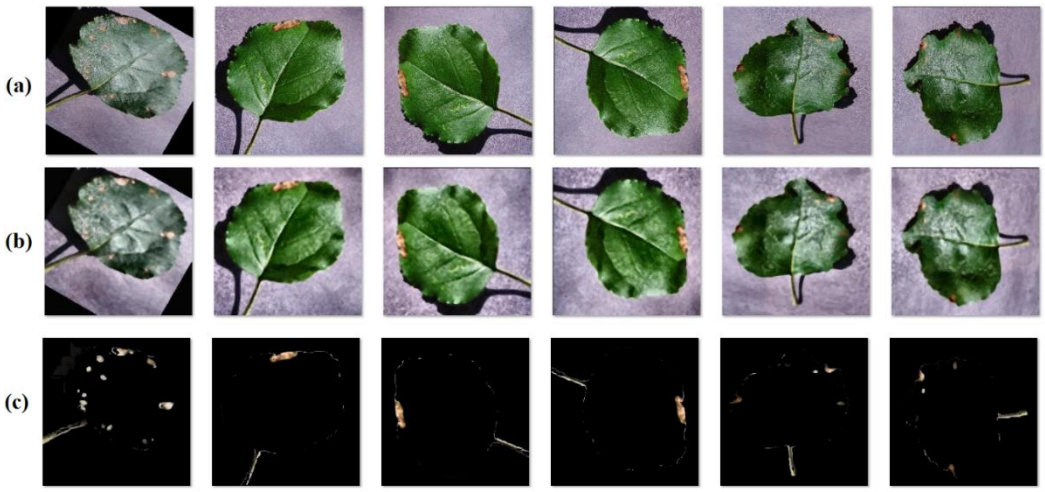

Figure 5. Sample results on Apple Dataset a) Original Images b) Pre-processed Images c) Segmented Images

A sample visualisation results analysis using the applied apple dataset and the suggested strategy is shown in Fig. 5. The original image, as well as the pre-processed and segmented versions of it, are displayed in Fig. 5a. The figures showed that the suggested model successfully pre-processed and segmented the images.

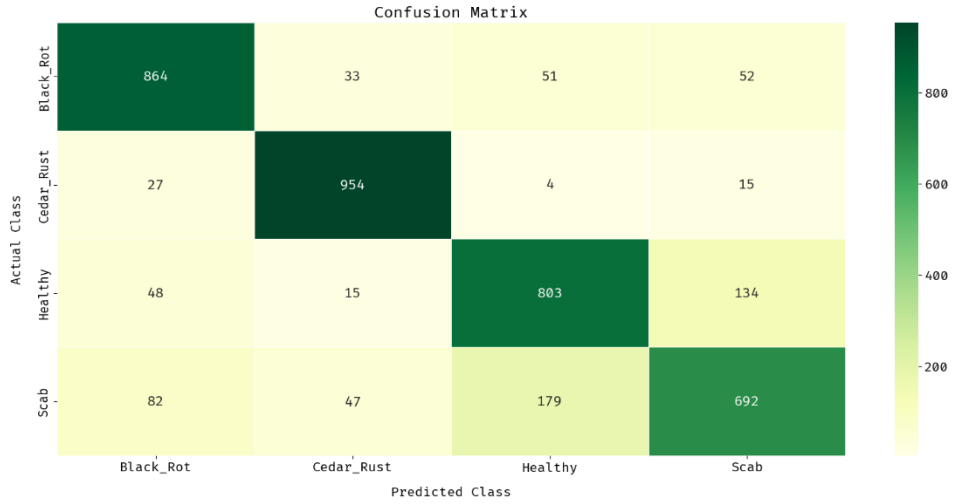

Figure 6. Confusion matrix analysis of DLEN-KLM model on apple plant disease dataset

Fig. 6 shows the confusion matrix generated by the DLEN-KLM method on the applicable dataset for apple plant disease. The results showed that a collection of 864 photos had been categorised using the DLEN-KLM technique as Black Rot, 954 images as Cedar Rust, 803 images as Healthy, and 692 images as Scab.

Table 1 Results of DLEN-KLM approach analysis on dataset of apple plant disease

Classes	Precision	Recall	Specificity	Accuracy	F-Score
Scab	0.8462	0.8640	0.9477	0.9268	0.8550
Healthy	0.9094	0.9540	0.9683	0.9648	0.9312
Cedar_Rust	0.7743	0.8030	0.9220	0.8922	0.7884
Black_Rot	0.7749	0.6920	0.9330	0.8728	0.7311
Average	**0.8262**	**0.8282**	**0.9428**	**0.9141**	**0.8264**

Table 1 and Fig. 7 exemplify the outcomes of the classification study performed using the DLEN-KLM method on the dataset pertaining to apple plant disease. The experimental outcomes denoted that the DLEN-KLM technique has effectively classified the images into distinct classes. For instance, with Scab class, the DLEN-KLM algorithm has classified the images with the prec. of 0.8462, rec. of 0.8640, specificity of 0.9477, acc. of 0.9268, and F-measure of 0.8550. Along with that, with Healthy class, the DLEN-KLM system has classified the images with the prec. of 0.9094, rec. of 0.9540, specificity of 0.9683, acc. of 0.9648, and F-measure of 0.9312. Followed by, with Cedar_Rust class, the DLEN-KLM manner has classified the images with the prec. of 0.7743, rec. of 0.8030, specificity of 0.9220, acc. of 0.8922, and F-measure of 0.7884. At last, with Black_Rot class, the DLEN-KLM algorithm has classified the images with the prec. of 0.7749, rec. of 0.6920, specificity of 0.9330, acc. of 0.8728, and F-measure of 0.7311.

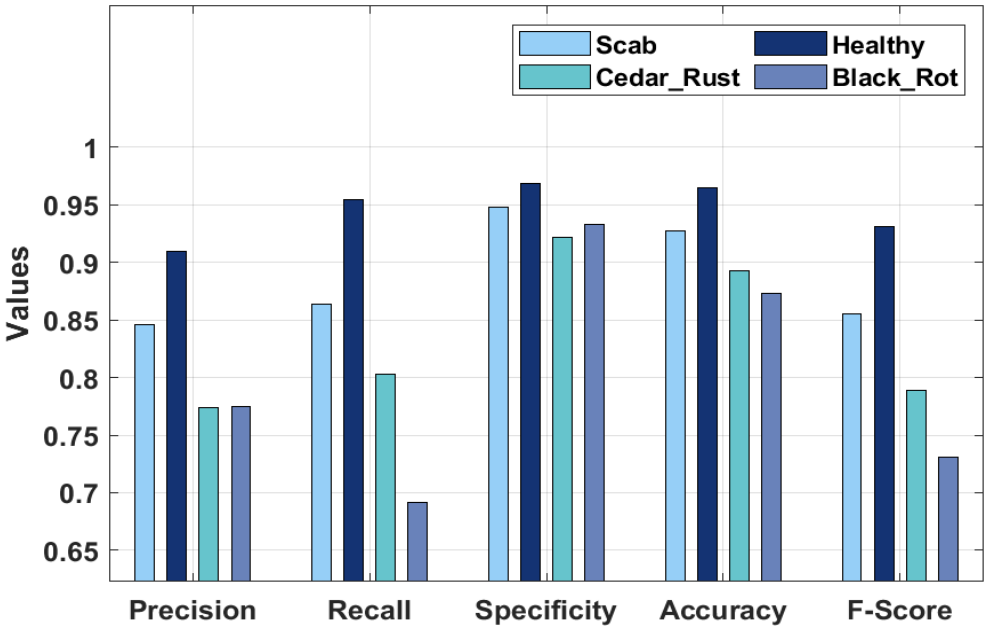

Figure 7. Result analysis of DLEN-KLM model with different measures

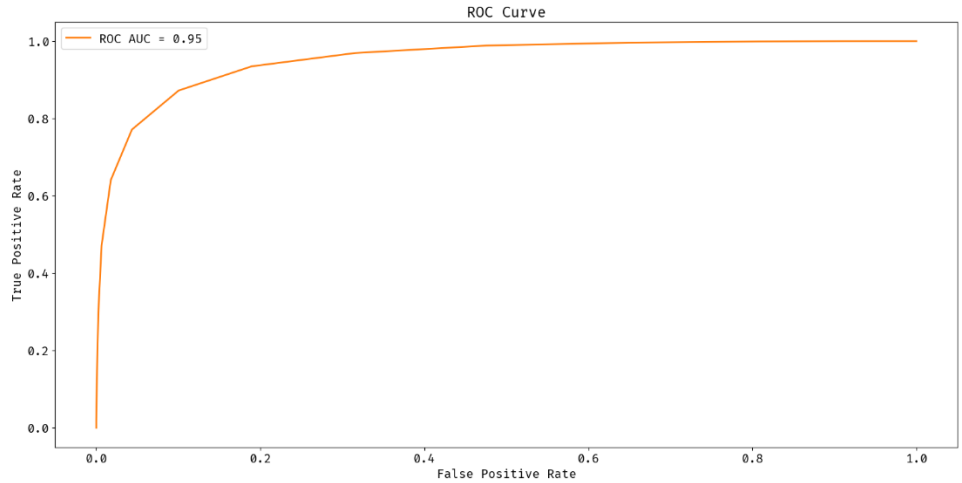

Figure 8. ROC of Apple Dataset on Proposed Model

Fig. 8 investigates the ROC analysis of the DLEN-KLM technique on the test apple plant disease dataset. The figure portrayed that the DLEN-KLM technique has accomplished effectual outcomes with a maximum AUC of 0.95.

Table 2 shows the accuracy comparison of the proposed DLEN-KLM model with currently used methods for the dataset for apple leaf disease.

Methods	Accuracy (%)
DLEN-KLM	91.41
MobileNet	73.50
InceptionV3	75.59
ResNet152	77.65
ROI-aware DCNN	84.30

In order to showcase the outstanding performance of the DLEN-KLM technique, a brief comparison study is made in Table 2 and Fig. 9 [23, 24]. The obtained results depicted that the DLEN-KLM technique has resulted in superior performance with an accuracy of 91.41% whereas the MobileNet, InceptionV3, ResNet152, and ROI-aware DCNN techniques have resulted in higher accuracy of 73.50%, 75.59%, 77.65%, and 84.30% respectively.

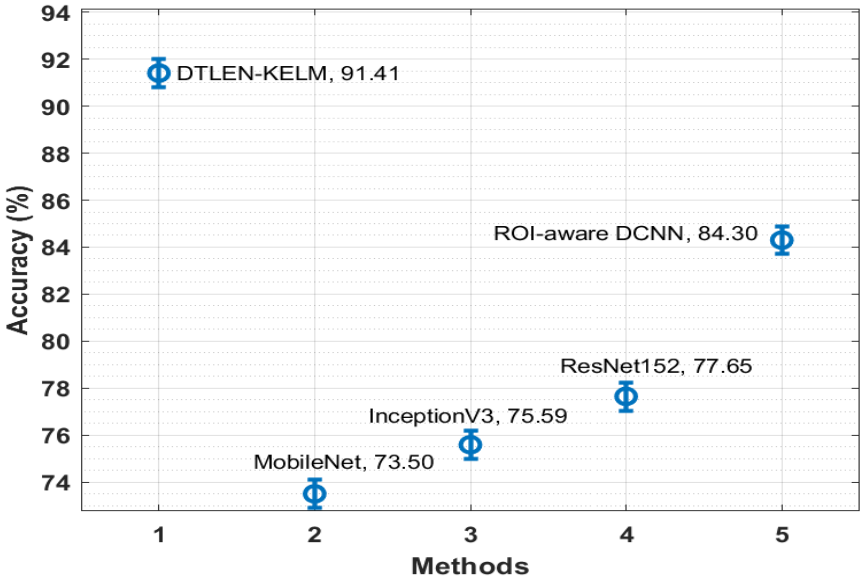

Figure 9. Accuracy analysis of DLEN-KLM model with existing techniques

4.2. Results of the Dataset on Potato Plant Disease

The proposed model's results analysis on the used dataset for potato pant disease are examined in this section.The test image samples from the dataset are shown in Fig. 10. A example visualisation results analysis using the suggested technique and the used potato dataset is shown in Fig. 11. The original image as well as its related pre-processed and segmented images are shown in Fig. 11a. The figures showed that the photos had been expertly pre-processed and split using the suggested technique.

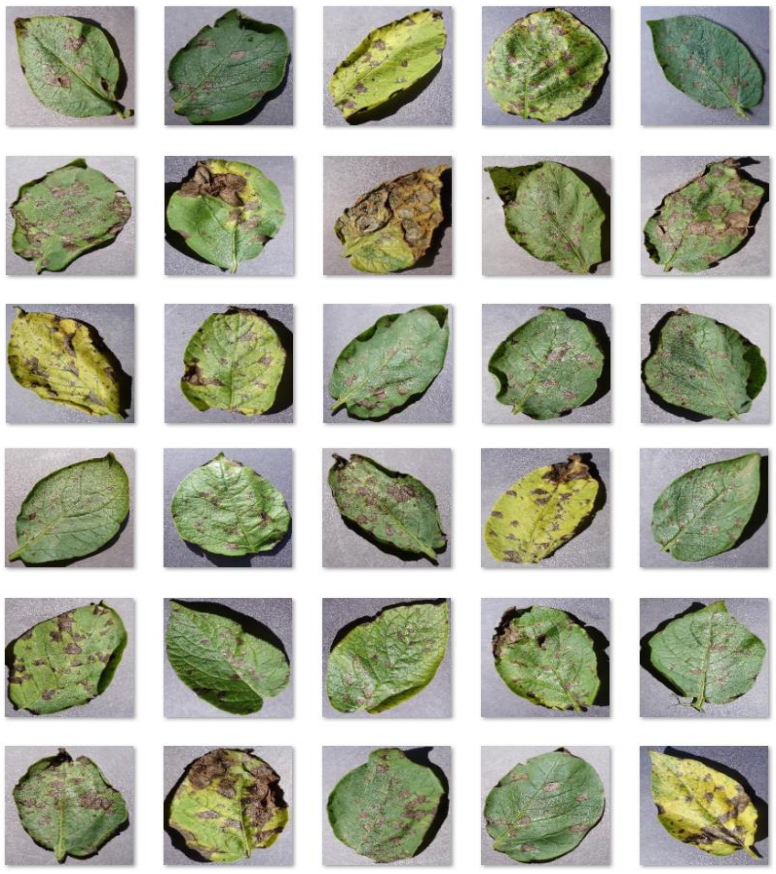

Figure 10. Sample Potato Plant Disease Images

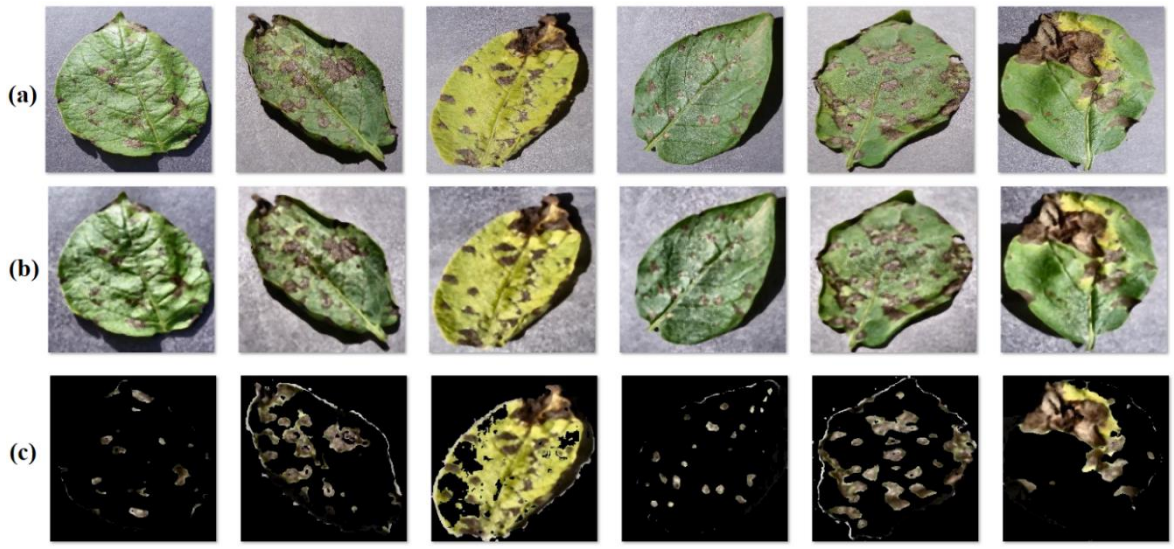

Figure 11. Potato Dataset a) Original Images b) Pre-processed Images c) Segmented Images

Fig. 12 displays the confusion matrix created by the DLEN-KLM approach on the dataset used to study potato plant disease. The outcomes exhibited that the DLEN-KLM technique has classified a set of 871 images under Early_Blight, 955 images under Healthy, and 828 images under Late_Blight.

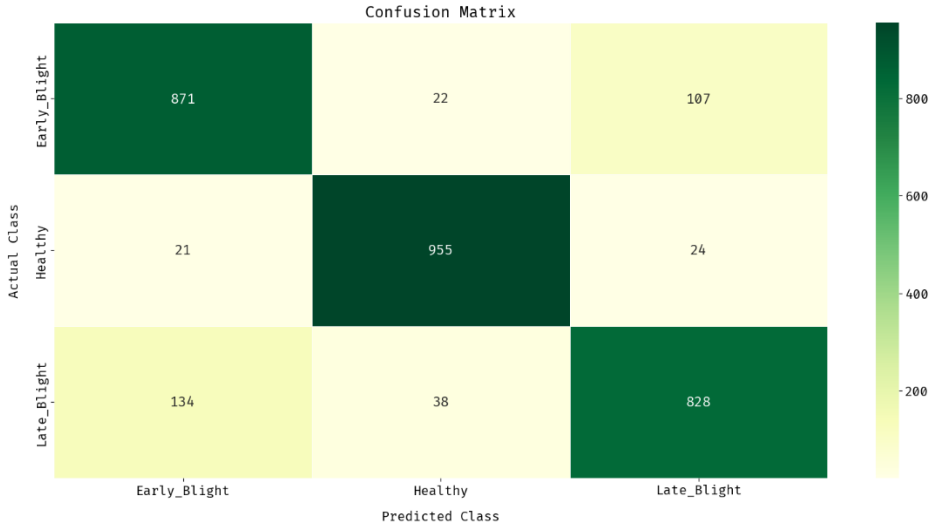

Figure 12. Confusion matrix analysis of DLEN-KLM model on potato plant disease dataset

Table 3 Results of DLEN-KLM approach analysis on dataset of potato plant disease

Classes	Precision	Recall	Specificity	Accuracy	F-Score
Early_Blight	0.8489	0.8710	0.9225	0.9053	0.8598
Healthy	0.9409	0.9550	0.9700	0.9650	0.9479
Late_Blight	0.8634	0.8280	0.9345	0.8990	0.8453
Average	**0.8844**	**0.8847**	**0.9423**	**0.9231**	**0.8843**

In Table 3 and Fig. 13, The DLEN-KLM method outperforms the categorization results analysis on the dataset for potato plant disease. The experimental outcomes represented that the DLEN-KLM approach has effectively classified the images into varying classes. For instance, with Early Blight class, the DLEN-KLM scheme has classified the images with the prec. of 0.8489, rec. of 0.8710, specificity of 0.9225, acc. of 0.9053, and F-measure of 0.8598.

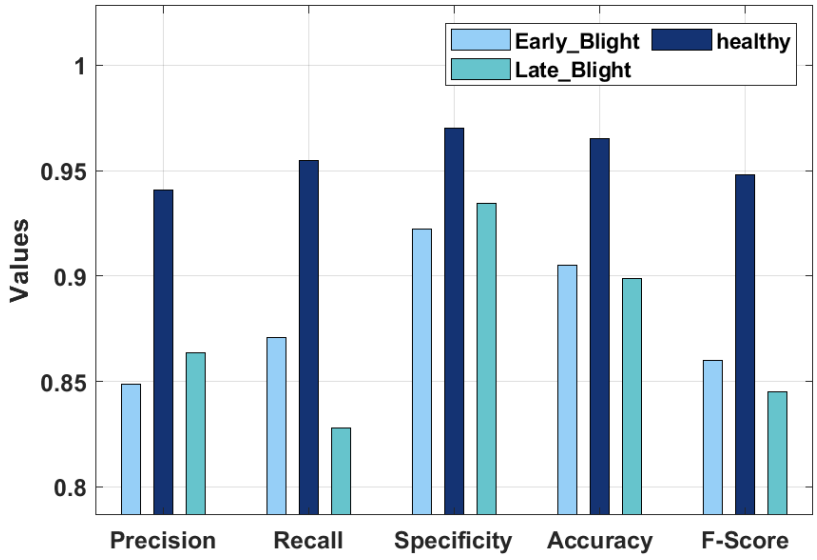

Figure 13. Result analysis of DLEN-KLM model

Besides, with Healthy class, the DLEN-KLM system has classified the images with the prec. of 0.9409, rec. of 0.9550, specificity of 0.9700, acc. of 0.9650, and F-measure of 0.9479. At least, with Late_Blight class, the DLEN-KLM technique has classified the images with the prec. of 0.8634, rec. of 0.8280, specificity of 0.9345, acc. of 0.8990, and F-measure of 0.8453.

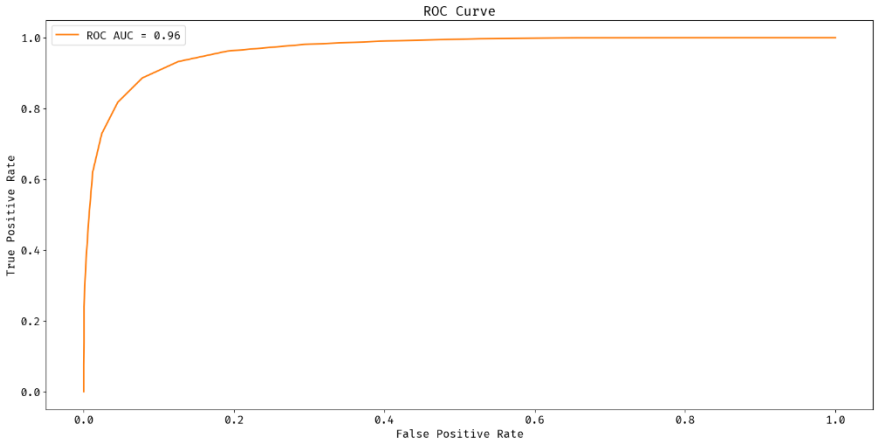

Figure 14. ROC of Potato Dataset on Proposed Model

Fig. 14 examines the ROC analysis of the DLEN-KLM approach on the test potato plant disease dataset. The figure outperformed that the DLEN-KLM methodology has accomplished effectual outcomes with the maximal AUC of 0.96.

Table 4 shows the accuracy comparison of the proposed DLEN-KLM model with currently used methods for the dataset for potato leaf disease.

Methods	Accuracy (%)
DLEN-KLM	93.31
CNN-SVM	85.18
CNN-RF	78.24
CNN-ANN	91.03
GoogleNet	83.00
VGGNet	84.26

A quick comparison analysis is done in Table 4 and Fig. 15 to show the DLEN-KLM algorithm's exceptional performance [25, 26]. The obtained resultant depicted that the DLEN-KLM methodology has resulted in higher performance with an accuracy of 92.31% whereas the CNN-SVM, CNN-RF, CNN-ANN, GoogleNet, and VGGNet techniques have resulted in increased accuracy of 84%, 79%, 92%, 86%, and 86% correspondingly.

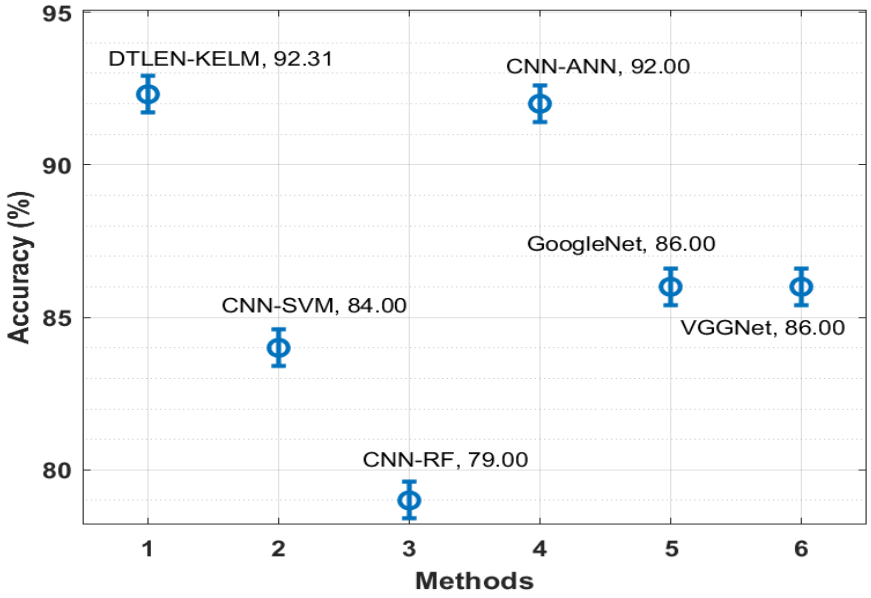

Figure 15. Accuracy analysis of DLEN-KLM model recent approaches

V. CONCLUSION

A new DLEN-KLM model is created in this study to identify and categorise plant diseases. The DLEN-KLM model consists of several subprocesses, including noise removal based on MF, contrast enhancement based on CLAHE, segmentation based on Otsu thresholding, feature extraction based on EfficientNet B0, and classification based on KLM. A benchmark dataset was used to validate the DLEN-KLM method's performance, and the findings were examined in relation to various evaluation criteria. The experimental findings demonstrated improved illness diagnosis over more contemporary methods. To further boost classification performance, the hyperparameters of the EfficientNet model can be adjusted in the future utilising metaheuristic methods.

REFERENCES

[1] Mohanty, S.P., Hughes, D.P. and Salathé, M., 2016. Using deep learning for image-based plant disease detection. *Frontiers in plant science*, *7*, p.1419.

[2] Ferentinos, K.P., 2018. Deep learning models for plant disease detection and diagnosis. *Computers and Electronics in Agriculture*, *145*, pp.311-318.

[3] Wang, G., Sun, Y. and Wang, J., 2017. Automatic image-based plant disease severity estimation using deep learning. *Computational intelligence and neuroscience*, *2017*.

[4] Türkoğlu, M. and Hanbay, D., 2019. Plant disease and pest detection using deep learning-based features. *Turkish Journal of Electrical Engineering & Computer Sciences*, *27*(3), pp.1636-1651.

[5] Barbedo, J.G.A., 2019. Plant disease identification from individual lesions and spots using deep learning. *Biosystems Engineering*, *180*, pp.96-107.

[6] Saleem, M.H., Potgieter, J. and Arif, K.M., 2019. Plant disease detection and classification by deep learning. *Plants*, *8*(11), p.468.

[7] Too, E.C., Yujian, L., Njuki, S. and Yingchun, L., 2019. A comparative study of fine-tuning deep learning models for plant disease identification. *Computers and Electronics in Agriculture*, *161*, pp.272-279.

[8] Verma, S., Chug, A., Singh, A.P., Sharma, S. and Rajvanshi, P., 2019. Deep learning-based mobile application for plant disease diagnosis: A proof of concept with a case study on tomato plant. In *Applications of Image Processing and Soft Computing Systems in Agriculture* (pp. 242-271). IGI Global.

[9] Nagaraju, M. and Chawla, P., 2020. Systematic review of deep learning techniques in plant disease detection. *International Journal of System Assurance Engineering and Management*, *11*(3), pp.547-560.

[10] Hernández, S. and Lopez, J.L., 2020. Uncertainty quantification for plant disease detection using Bayesian deep learning. Applied Soft Computing, 96, p.106597.

[11] Guo, Y., Zhang, J., Yin, C., Hu, X., Zou, Y., Xue, Z. and Wang, W., 2020. Plant disease identification based on deep learning algorithm in smart farming. Discrete Dynamics in Nature and Society, 2020.
[12] Saleem, M.H., Khanchi, S., Potgieter, J. and Arif, K.M., 2020. Image-based plant disease identification by deep learning meta-architectures. Plants, 9(11), p.1451.
[13] Kabir, M.M., Ohi, A.Q. and Mridha, M.F., 2021. A Multi-Plant Disease Diagnosis Method using Convolutional Neural Network. In Computer Vision and Machine Learning in Agriculture (pp. 99-111). Springer, Singapore.
[14] Hong, H., Lin, J. and Huang, F., 2020, June. Tomato disease detection and classification by deep learning. In 2020 International Conference on Big Data, Artificial Intelligence and Internet of Things Engineering (ICBAIE) (pp. 25-29). IEEE.
[15] Patil, B.V. and Patil, P.S., 2021. Computational method for Cotton Plant disease detection of crop management using deep learning and internet of things platforms. In Evolutionary Computing and Mobile Sustainable Networks (pp. 875-885). Springer, Singapore.
[16] Lijo, J., 2021, April. Analysis of Effectiveness of Augmentation in Plant Disease Prediction using Deep Learning. In *2021 5th International Conference on Computing Methodologies and Communication (ICCMC)* (pp. 1654-1659). IEEE.
[17] Turkoglu, M., Yanikoğlu, B. and Hanbay, D., 2021. PlantDiseaseNet: convolutional neural network ensemble for plant disease and pest detection. Signal, Image and Video Processing, pp.1-9.
[18] Zhu, Y. and Huang, C., 2012. An improved median filtering algorithm for image noise reduction. *Physics Procedia*, *25*, pp.609-616.
[19] Xu, X., Xu, S., Jin, L. and Song, E., 2011. Characteristic analysis of Otsu threshold and its applications. *Pattern recognition letters*, *32*(7), pp.956-961.
[20] Atila, Ü., Uçar, M., Akyol, K. and Uçar, E., 2021. Plant leaf disease classification using EfficientNet deep learning model. *Ecological Informatics*, *61*, p.101182.
[21] Chen, C., Li, W., Su, H. and Liu, K., 2014. Spectral-spatial classification of hyperspectral image based on kernel extremelearning machine. *Remote sensing*, *6*(6), pp.5795-5814.
[22] https://www.kaggle.com/vipoooool/new-plant-diseases-dataset/data#
[23] Bi, C., Wang, J., Duan, Y., Fu, B., Kang, J.R. and Shi, Y., 2020. MobileNet based apple leaf diseases identification. *Mobile Networks and Applications*, pp.1-9.
[24] Yu, H.J., Son, C.H. and Lee, D.H., 2020. Apple leaf disease identification through region-of-interest-aware deep convolutional neural network. *Journal of Imaging Science and Technology*, *64*(2), pp.20507-1.
[25] Samer I. Mohamed, Potato Leaf Disease Diagnosis and Detection System Based on Convolution Neural Network, International Journal of Recent Technology and Engineering (IJRTE) ISSN: 2277-3878, Volume-9 Issue-4, November 2020.
[26] Afzaal, H., Farooque, A.A., Schumann, A.W., Hussain, N., McKenzie-Gopsill, A., Esau, T., Abbas, F. and Acharya, B., 2021. Detection of a potato disease (early blight) using artificial intelligence. *Remote Sensing*, *13*(3), p.411.